Electronic Supplementary Information

Synthesis of Z-scheme Cobalt Porphyrin/Nitrogen-doped Graphene Quantum Dot Heterojunctions for Efficient Molecule-based Photocatalytic Oxygen Evolution

*Zhou Zhong,[a,c] Jingjing Liu,[**b] Xiao Xu,[a] Aihui Cao, [a,c] Zhijie Tao, [a] Weifeng You, [a,c] and Longtian Kang*[a]*

[a] Key Laboratory of Design and Assembly of Functional Nanostructures, and Fujian Provincial Key Laboratory of Nanomaterials, Fujian Institute of Research on the Structure of Matter, Chinese Academy of Sciences, Fuzhou, Fujian 350002, P. R. China.

[b] Fujian Universities and Colleges Engineering Research Center of Soft Plastic Packaging Technology for Food, School of Ocean and Biochemical Engineering, Fuqing Branch of Fujian Normal University, Fuqing, Fujian Province, 350300, P. R. China..

[c] University of Chinese Academy of Sciences, Chinese Academy of Sciences, Beijing, 100049, P. R. China.

* Corresponding author at: Fujian Institute of Research on the Structure of Matter, Chinese Academy of Sciences, Fuzhou, Fujian 350002, P. R. China. E-mail: longtiank@fjirsm.ac.cn

** Corresponding author at: Fuqing Branch of Fujian Normal University, Fuqing, Fujian Province, 350300, P. R. China. E-mail: 116425543@qq.com

Materials

Cobalt tetraphenylporphyrin (98%), citric acid monohydrate (99%) and ethylene diamine hydrochloride (99%) were purchased from Aladdin Industrial Incorporation. Iodine (99%), silver perchlorate (99%), anhydrous CH_2Cl_2 and anhydrous acetonitrile were from J&K Chemicals Co. Ltd. DMF, $FeSO_4 \cdot 7H_2O$ (analytical pure) and $AgNO_3$ (analytical pure) were obtain from Sinopharm Chemical Reagent Co., Ltd.

Instruments. The morphology and high-resolution transmission electron microscope (HRTEM) image of the samples was observed by SU-8010 field emission scanning electron microscope (FE-SEM) and Tecnai G2 F20 transmission electron microscopy (TEM) respectively. Powder X-ray diffraction (PXRD) data of the sample were collected by MiniFlex 600 diffractometer which is equipped with Cu Kα radiation. X-ray photoelectron spectroscopy (XPS) measurements were carried out on ESCALAB 250Xi spectrometer. UV-vis absorption and solid absorption spectra were recorded on Shimadzu UV2600 spectrophotometer. Photoluminescence (PL) spectra were obtained by Hitachi F-4600 spectrometer. All of the electrochemical and photoelectrochemical tests were conducted on a CHI 760E electrochemical workstation (Chen Hua Instruments, Shanghai, China). The experiments of photocatalytic water oxidation reaction were carried out in a closed gas circulation and evacuation system (Beijing PerfectLight, Labsolar-6A) using a 300W Xe lamp (Beijing PerfectLight, PLS-SXE300BF) as light source, and the evolved amount of O_2 was analysed by an on-line gas chromatograph (Techcomp, GC7900).

Femtosecond Transient Absorption (fsTA) Experiments

The fsTA measurements were performed through a femtosecond Ti:Sapphire regenerative amplified Ti:sapphire laser system (Spectra Physics, Spitfire-Pro) and a corresponding data acquisition system (Ultrafast Systems, Helios model). The excitation pulse (1 kHz, 240-2,600 nm, pulse width, 120 fs) was generated by an optical parametric amplifier (TOPAS-C, Spectra-Physics) pumped by a regeneratively amplified femtosecond Ti:sapphire laser system (800 nm, 1 kHz, pulse energy 4 mJ,

pulse width, 120 fs, Spitfire Pro-F1KXP, Spectra-Physics), which was seeded by a femtosecond Ti-sapphire oscillator (80 MHz, pulse width, 70 fs, 710-920 nm, Maitai XF-1, Spectra-Physics). The probe pulse was obtained by using approximately 5% of the amplified 800 nm output from the Spitfire to generate a white-light continuum (450-800 nm) in a sapphire plate. The maximum extent of the temporal delay was 3300 ps. The instrument response function was determined to be 150 fs. At each temporal delay, data were averaged for 2 s and collected by the acquisition system. The probe beam was split into two before passing through the sample. One probe beam traveled through the sample, the other was sent directly to the reference spectrometer that monitored the fluctuations in the probe beam intensity. Fiber optics was coupled to a multichannel spectrometer with a CMOS sensor that had a 1.5 nm intrinsic resolution. The sample suspension was excited by a 400 nm pump beam. The data were stored as three-dimensional (3D) wavelength-time-absorbance matrices that were exported for use with the fitting software.

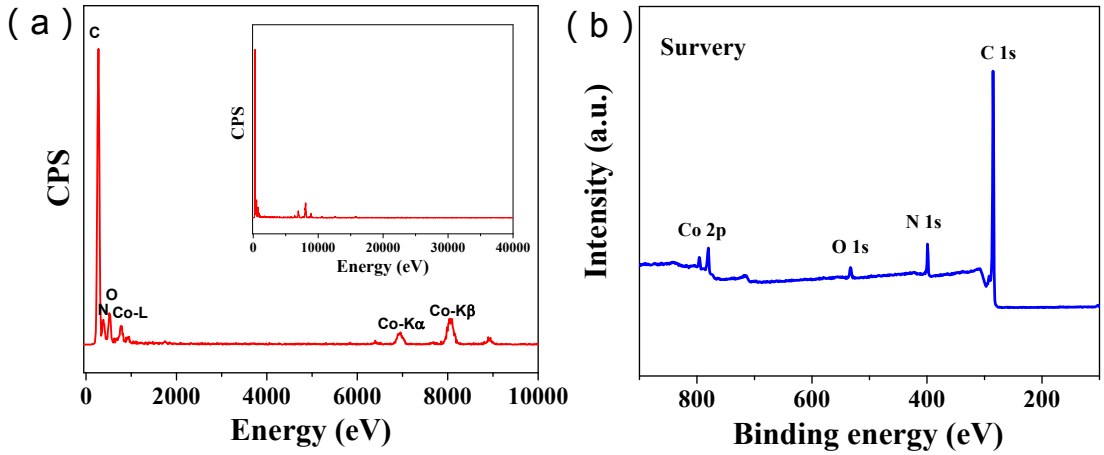

Fig. S1 (a) EDS and (b) XPS survery of CoP NWs.

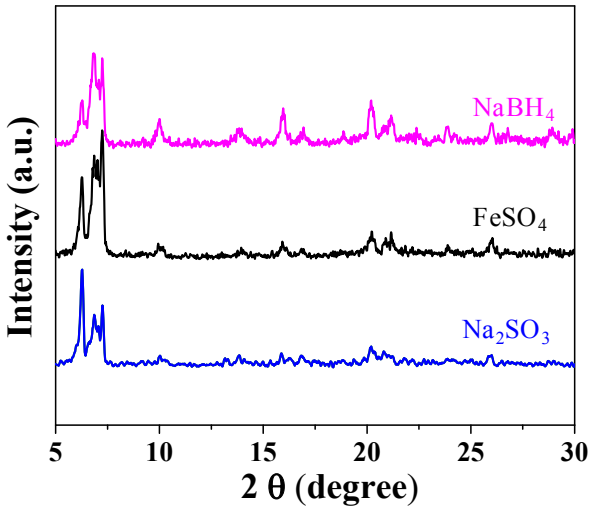

Fig. S2 (a) PXRD patterns of CoP NWs obtained with $NaBH_4$, $FeSO_4$ and Na_2SO_3 as reductant, respectively.

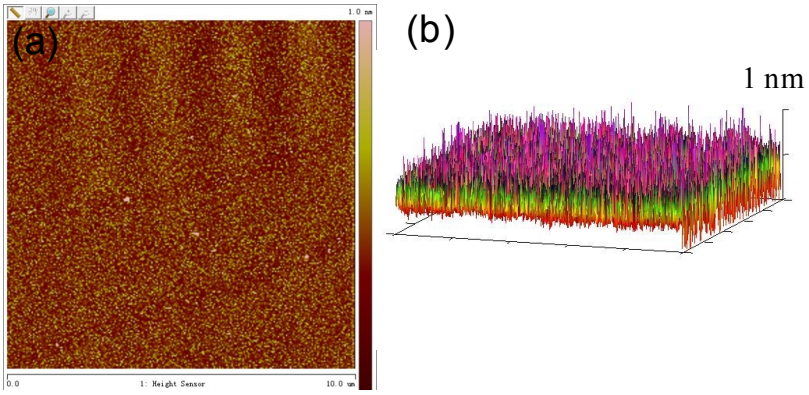

Fig. S3 (a) AFM image and (b) height distribution of NGQDs.

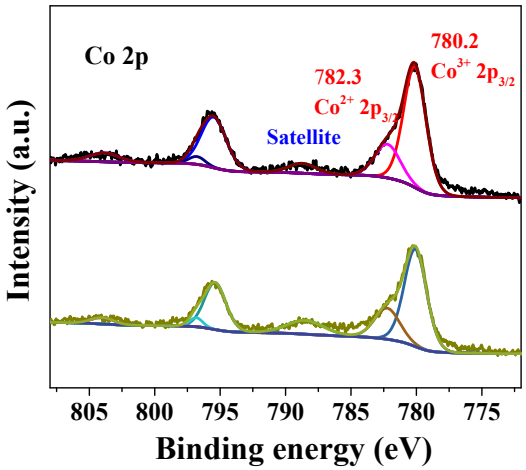

Fig. S4 High-resolution XPS spectra of Co 2p in CoP NWs and CoP/NGQDs NCs.

Fig. S5 $Fe(OH)_3$ NPs attached on CoP NWs.

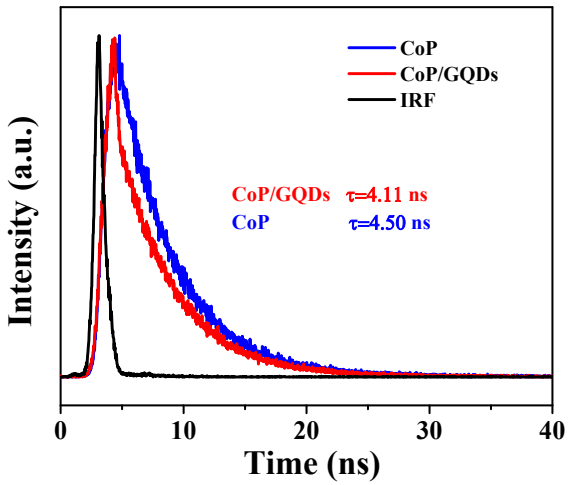

Fig. S6 Time-resolved fluorescence spectrum of CoP NWs and CoP/NGQDs NCs at 620 nm.

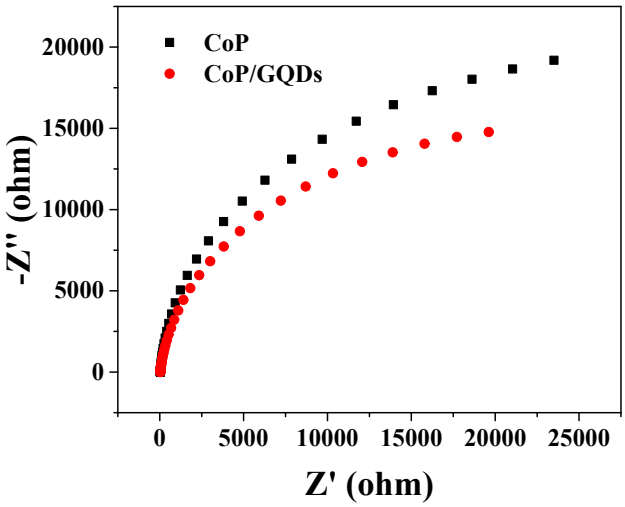

Fig. S7 Electrochemical impedance spectroscopy of CoP NWs and CoP/NGQDs NCs.

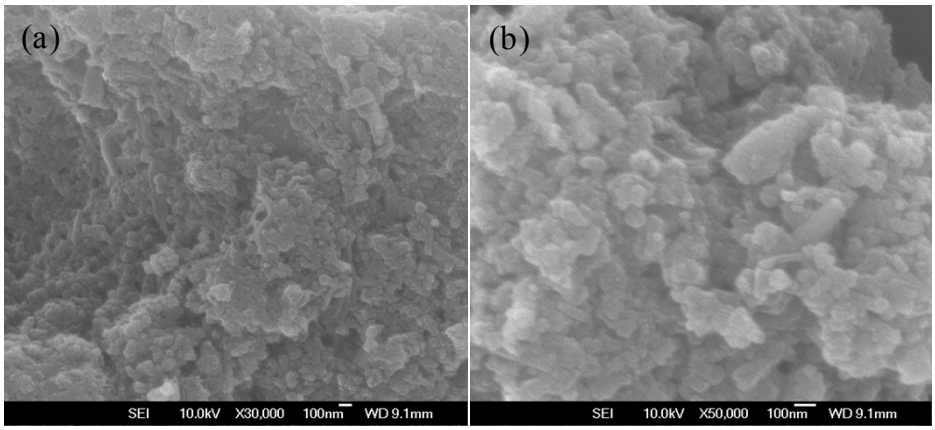

Fig. S8 SEM images of CoP/NGQDs NCs before/after POE test.

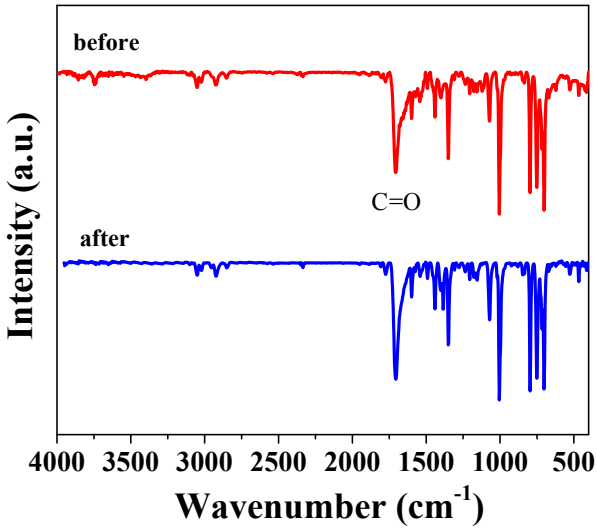

Fig. S9 FT-IR spectra of CoP/NGQDs NCs before/after POE test.

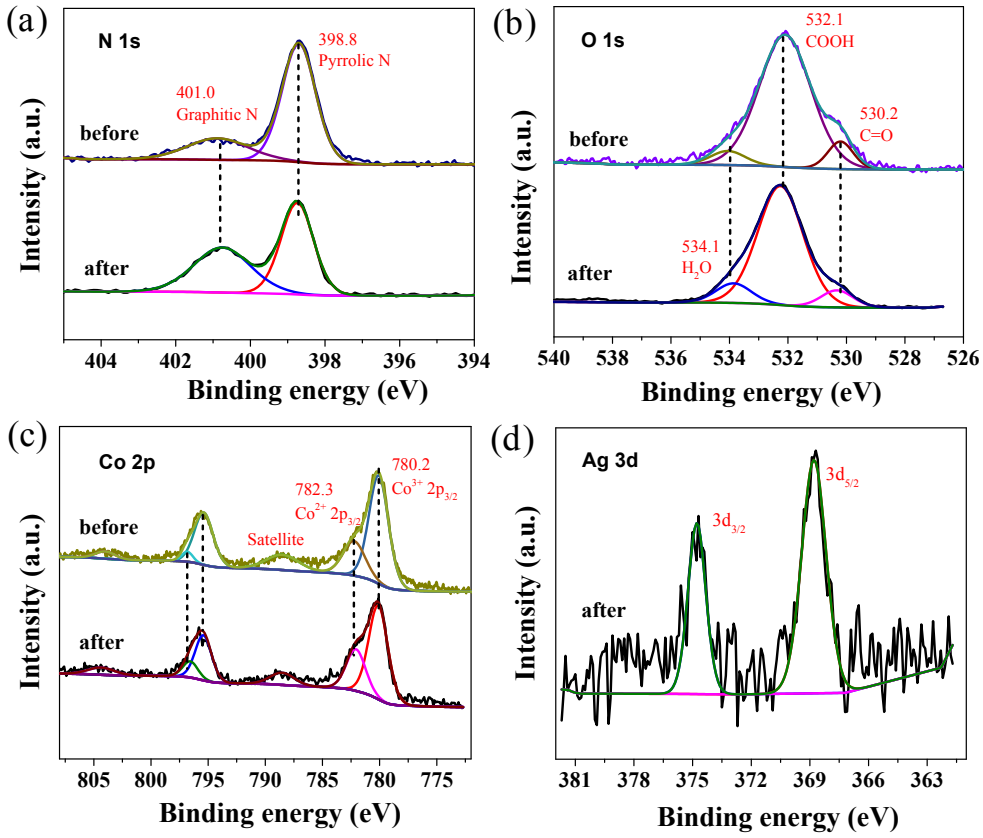

Fig. S10 High-resolution XPS of (a) N 1s, (b) O 1s, (c) Co 2p and (d) Ag 3d of CoP/NGQDs NCs before/after POE test.

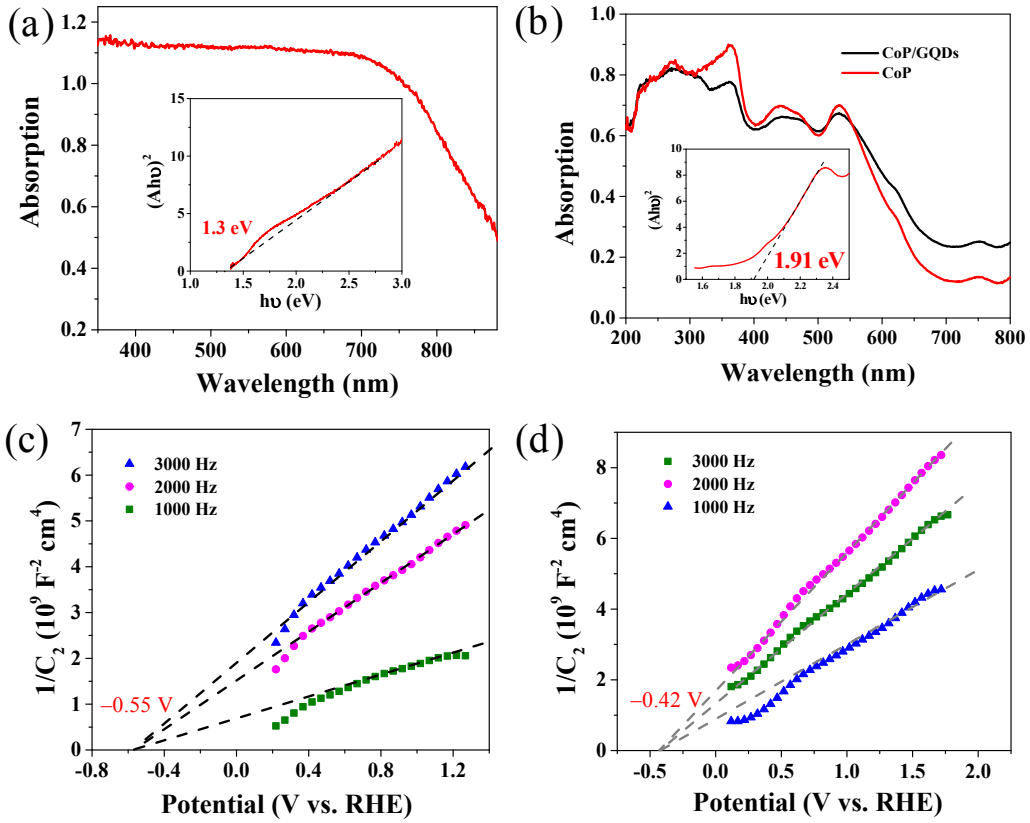

Fig. S11 Solid UV-vis absorption spectrum and the corresponding bandgap of (a) NGQDs and (b) CoP NWs. Mot-Schottky plots of (c) GQDs and (d) CoP NWs.

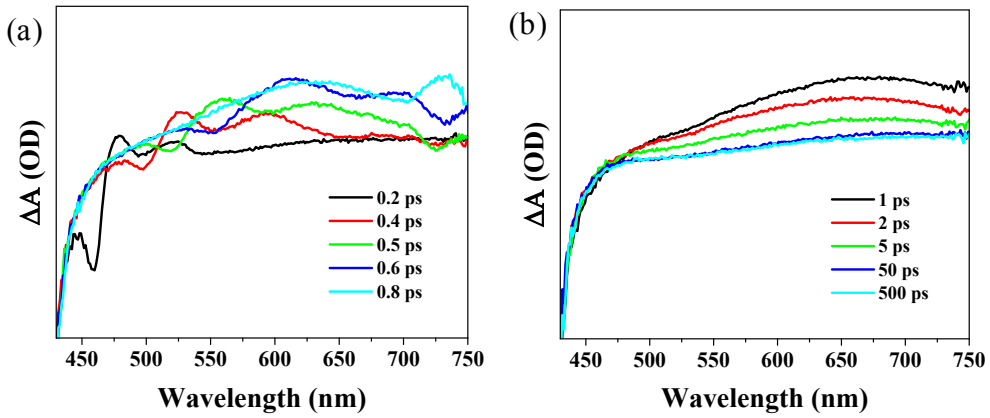

Fig. S12 The fsTA spectra of NGQDs.

Table S1 Comparison of POE activity of the molecule-based heterogeneous photocatalysts. Homogeneous photocatalysts and photocatalytic system needs photosensitizer such as $[Ru(bpy)_3]Cl_2$ are not included in the comparison

Photocatalyst	Sacrificial agent	Irradiation light	POE rate ($\mu mol\ g^{-1}\ h^{-1}$)	Reference
CoP/NGQDs	$AgNO_3$	λ>420 nm	350	This work
Tetra(4-carboxylphenyl)porphyrin	$AgNO_3$	300<λ<700	36.1	Ref. 1
2D tetraphenylporphyrin cobalt(II)	$AgNO_3$	λ>420 nm	43.3	Ref. 2
H_2TCPP NRs	$AgNO_3$	full spectrum	6.1	Ref. 3
PDI nanofibers	$AgNO_3$	λ>420 nm	30	Ref. 4
PDINH supramolecular	$AgNO_3$	λ>420 nm	2.58	Ref. 5
Ag_2S/PDI	$AgNO_3$	full spectrum	34.6	Ref. 6
PTCDA/g-C_3N_4	$AgNO_3$	λ>420 nm	17.3	Ref. 7
TCNQ-PTCDI	$AgNO_3$	λ>420 nm	14	Ref. 8
PTCDI-C_{60}	$AgNO_3$	λ>420 nm	22.5	Ref. 9
Bi_2WO_6/PDI	$AgNO_3$	λ>420 nm	7.5	Ref. 10

References

1. Z. Zhang, Y. Zhu, X. Chen, H. Zhang and J. Wang, *Adv. Mater.*, 2019, **31**, 1806626.

2. K. C. Ranjeesh, L. George, V. C. Wakchaure, Goudappagouda, R. N. Devi and S. S. Babu, *Chem. Commun.*, 2019, **55**, 1627-1630.

3. J. Meng, P. Bi, J. Jia, X. Sun and R. Chen, *ChemistrySelect*, 2017, **2**, 4882-4888.

4. J. Wang, W. Shi, D. Liu, Z. Zhang, Y. Zhu and D. Wang, *Appl. Catal. B:Environ.*, 2017, **202**, 289-297.

5. D. Liu, J. Wang, X. Bai, R. Zong and Y. Zhu, *Adv. Mater.*, 2016, **28**, 7284-7290.

6. J. Yang, H. Miao, W. Li, H. Li and Y. Zhu, *J. Mater. Chem. A*, 2019, **7**, 6482-6490.

7. Y.-J. Yuan, Z.-K. Shen, P. Wang, Z. Li, L. Pei, J. Zhong, Z. Ji, Z.-T. Yu and Z. Zou, *Appl. Catal. B:Environ.*, 2020, **260**, 118179.

8. Z. Zhang, J. Wang, D. Liu, W. Luo, M. Zhang, W. Jiang and Y. Zhu, *ACS Appl. Mater. Interfaces*, 2016, **8**, 30225-30231.

9. Y. Wei, M. Ma, W. Li, J. Yang, H. Miao, Z. Zhang and Y. Zhu, *Appl. Catal. B:Environ.*, 2018, **238**, 302-308.

10. K. Zhang, J. Wang, W. Jiang, W. Yao, H. Yang and Y. Zhu, *Appl. Catal. B:Environ.*, 2018, **232**, 175-181.